Therapeutics and Clinical Risk Management

Dovepress

open access to scientific and medical research

Open Access Full Text Article

ORIGINAL RESEARCH

Comparative Effectiveness of MRI, 4D-CT and Ultrasonography in Patients with Secondary Hyperparathyroidism

Jiaoping Mi[1,2,*], Yijie Fang[3,*], Jianzhong Xian[4], Guojie Wang[3], Yuanqing Guo[5], Haiyu Hong[2], Mengshi Chi[2], Yong-Fang Li[2], Peng He[2], Jiebing Gao[3], Wei Liao[2]

[1]Department of Otolaryngology Head and Neck Surgery, The First Affiliated Hospital of Sun Yat-sen University, Zhuhai, Guangdong, People's Republic of China; [2]Department of Otolaryngology Head and Neck Surgery, The Fifth Affiliated Hospital of Sun Yat-sen University, Zhuhai, Guangdong, People's Republic of China; [3]Department of Radiology, The Fifth Affiliated Hospital of Sun Yat-sen University, Zhuhai, Guangdong, People's Republic of China; [4]Department of Ultrasound, The Fifth Affiliated Hospital of Sun Yat-sen University, Zhuhai, Guangdong, People's Republic of China; [5]Department of Spinal Surgery, The Fifth Affiliated Hospital of Sun Yat-sen University, Zhuhai, Guangdong, People's Republic of China

*These authors contributed equally to this work

Correspondence: Wei Liao, Department of Otolaryngology Head and Neck Surgery, The Fifth Affiliated Hospital of Sun Yat-sen University, Zhuhai, Guangdong, 519020, People's Republic of China, Email liaowei23@mail.sysu.edu.cn; Jiebing Gao, Department of Radiology, The Fifth Affiliated Hospital of Sun Yat-sen University, Zhuhai, Guangdong, People's Republic of China, Email Gaojb@mail.sysu.edu.cn

Objective: Accurate preoperative localization of abnormal parathyroid glands is crucial for successful surgical management of secondary hyperparathyroidism (SHPT). This study was conducted to compare the effectiveness of preoperative MRI, 4D-CT, and ultrasonography (US) in localizing parathyroid lesions in patients with SHPT.

Methods: We performed a retrospective review of prospectively collected data from a tertiary-care hospital and identified 52 patients who received preoperative MRI and/or 4D-CT and/or US and/or ^{99m}Tc-MIBI and subsequently underwent surgery for SHPT between May 2013 and March 2020. The sensitivity, specificity, positive predictive value (PPV) and negative predictive value (NPV) of each imaging modality to accurately detect enlarged parathyroid glands were determined using histopathology as the criterion standard with confirmation using the postoperative biochemical response.

Results: A total of 198 lesions were identified intraoperatively among the 52 patients included in this investigation. MRI outperformed 4D-CT and US in terms of sensitivity ($P < 0.01$), specificity ($P = 0.455$), PPV ($P = 0.753$), and NPV ($P = 0.185$). The sensitivity and specificity for MRI, 4D-CT, and US were 90.91%, 88.95%, and 66.23% and 58.33%, 63.64%, and 50.00%, respectively. The PPV of combined MRI and 4D-CT (96.52%) was the highest among the combined 2 modalities. The smallest diameter of the parathyroid gland precisely localized by MRI was 8×3 mm, 5×5 mm by 4D-CT, and 5×3 mm by US.

Conclusion: MRI has superior diagnostic performance compared with other modalities as a first-line imaging study for patients undergoing renal hyperparathyroidism, especially for ectopic or small parathyroid lesions. We suggest performing US first for diagnosis and then MRI to make a precise localization, and MRI proved to be very helpful in achieving a high success rate in the surgical treatment of renal hyperparathyroidism in our own experience.

Keywords: MRI, 4D-CT, ultrasonography, SHPT, preoperative localization, parathyroidectomy

Introduction

Secondary renal hyperparathyroidism (SHPT) is a common complication of chronic renal failure (CRF) that injures multiple systems in the body[1] and poses a severe threat to patients' lives and quality of life.[2,3] Parathyroidectomy is an effective method for patients who are unresponsive to medical therapy. The parathyroid gland location can vary considerably due to its complex embryologic descent from the third and fourth pharyngeal pouches. Moreover, ectopic glands can be found in the superior mediastinum, carotid sheath, retroesophageal location, thymus, or thyroid

Received: 16 July 2022
Accepted: 13 February 2023
Published: 2 May 2023

parenchyma itself.[4] Therefore, accurate preoperative localization of abnormal parathyroid glands is crucial for more rapid and appropriate surgery, especially in high-risk patients with kidney failure.[5]

Cervical ultrasonography (US) and 99mTc-sestamibi (MIBI) scintigraphy are used most commonly. However, the sensitivity of US in detecting parathyroid adenomas can vary considerably (51% to 90%) according to the ultrasonographer.[6,7] The location, gland size, hyperplasia type and presence of thyroid disease in patients with parathyroid glands were reported to be important factors influencing the MIBI biphasic image.[8] In 2006, 4-dimensional computed tomography (4D-CT) emerged as another option. It can visualize critical anatomical and functional information in short order, even detecting some supernumerary and ectopic parathyroid glands.[9,10] More recently, magnetic resonance imaging (MRI) has been utilized in parathyroid disease, such as parathyroid and recurrent or persistent postoperative primary hyperparathyroidism.[11,12] Despite this present trend, very few studies have assessed these modalities in a head-to-head comparison, and it is not known whether preoperative attempts at localization of parathyroid glands in patients with expected 4-gland hyperplasia are beneficial.

Although there is much controversy about the use of preoperative imaging methods, it is absolutely important to use preoperative imaging if surgery is to be rapidly performed. The purpose of the current study was to compare the effectiveness of the 4 preoperative localizing imaging modalities (MRI, 4D-CT, US and ^{99m}Tc- MIBI) in a large population of patients with SHPT.

Materials and Methods

We performed a retrospective analysis of the collected database from the Fifth Affiliated Hospital of Sun Yat-sen University. The Institutional Review Board approved the study protocol. This study fully complied with the Declaration of Helsinki and was accredited by the ethical board of The Fifth Affiliated Hospital of Sun Yat-sen University. Secondary hyperparathyroidism was diagnosed by means of elevated serum parathyroid hormone (PTH) levels using an immunoradiometric assay for intact PTH (pmol/L), documented enlarged parathyroid glands at surgery, and confirmation by histopathology.

Patients

Between May 2013 and March 2020, we identified 52 patients, 18 years of age or older, with secondary renal hyperparathyroidism from outpatients or inpatients. All patients received preoperative 4D-CT and/or MRI and/or US [10 patients also received ^{99m}Tc-MIBI]. All images were reviewed independently and blindly by two senior radiologists and ultrasonologists who had extensive experience with this technique.

Preoperative Localization Techniques

High-Resolution Ultrasonography

Ultrasonography was performed by an experienced radiologist with 7–12 MHz linear transducers (iU22; Philips, Andover, Mass) for cervical examination over a field extending from the clavicles to the mandible in a supine position with the neck extended and the shoulder lowered. The upper mediastinum was studied by using an endocavitary probe with a frequency of 4.5–7.2 MHz for retrosternal exploration. In addition to identification of the involved parathyroid glands, the thyroid parenchyma was also studied. The radiologist was asked to score the presence of hyperplastic parathyroid gland(s) for each possible location (on the right and left sides, superior and inferior glands, and potential ectopic glands). The size of each gland (largest measurement) was measured. Equivocal images were considered negative.

^{99m}Tc-sestaMIBI Scintigraphy

Anterior planar images of the neck and chest were obtained for 5 minutes in a 256×256 matrix at intervals of 15 min and 2 h following the injection of 800 MBq 99mTc-sestaMIBI using a dual-headed gamma camera (Symbia T16; Siemens, Erlangen, Germany). Any focus of abnormal tracer uptake with retention on delayed imaging in the region of the thyroid bed or any potential site for ectopic hyperfunctioning glands was interpreted as a positive study for hyperplastic parathyroid glands. Equivocal images were considered negative.

4D-CT Scanning

All 4D-CT scans were performed with a second-generation, 128-section, dual-energy CT scanner (Somatom Definition Flash unit, Siemens Healthcare, Forchheim, Germany). All patients were scanned from the angle of the mandible to the carina. The 4D-CT protocol was scanned in dual-energy mode, including nonenhanced images and arterial and venous phase image series. The parameters are as follows: two tube voltages of 80 kV (tube A) and Sn140 kV (tube B), reference current-time product of 255 mAs (tube A) and 60 mAs (tube B), with automated attenuation-based tube current modulation (Care Dose 4D, Siemens Healthcare), collimation of 64×0.6 mm, pitch of 0.7, and rotation time of 0.28 s. The arterial and venous phase scanning began automatically at 10s and 35s after the left common carotid artery reached the trigger attenuation threshold (100 HU) using automated scan-triggering software (CARE Bolus CT; Siemens Healthineers). The volume of iodinated contrast material (iohexol, Omnipaque 300; GE Healthcare, Piscataway, SH) was 70 mL. The mean dual-source CT dose index volume was 34.5 mGy, which was comparable to a CT dose index volume of 41.8 mGy for conventional neck scanning in patients with normal body mass indices at our institution.

MR Imaging

All MR imaging was performed with a 3.0T scanner (Siemens Magnetom Verio, Siemens Medical Solutions, USA) with a dedicated four-channel neurovascular phased array coil. The T2-weighted turbo inversion recovery magnitude was performed in the coronal plane. The T1-weighted and T2-weighted sequences with Dixon fat saturation were performed in the axial plane, and axial DWI multishot echo-planar sequences (RESOLVE) were also performed in the axial plane. The imaging parameters are shown in Table 1.

Surgery

All 4 imaging studies were performed within a 2-week interval of each other. All patients underwent total parathyroidectomy plus autologous transplantation (tPTX+AT). The hyperparathyroid tissue was removed and then confirmed via intraoperative rapid freezing pathological examination, and the final histopathologic diagnosis was obtained. Autologous transplantation was not performed if fewer than 4 pieces of hyperparathyroid tissue were removed. The sensitivity, specificity, positive predictive value and negative predictive value of the imaging modalities were determined from the combined information from all patients.

Statistical Analysis

The results of imaging examinations, which were read independently, were evaluated for each gland with reference to surgical exploration and histopathologic specimens. We calculated on a per-lesion analysis of each modality through pathology (top left, top right, bottom left, bottom right or ectopic). An abnormal image or focus was classified either as a true-positive (TP) result if it corresponded to an abnormal parathyroid gland if it was on the same side of the thyroid bed or in an ectopic position, or as a false-negative (FP) result if it did not. If no abnormal image or focus was reported in a site, the presence of any abnormal gland was considered a false-negative (FN) result; a result was considered true-negative T (TN) in a site only if the gland(s) was (were) normal or if no gland was found at surgery. Data were analyzed

Table 1 Specific MR Pulse Sequence Parameters

	T1-DIXON	T2-DIXON	T2-TIRM	RESOLVE-DW
Acquisition plane	Axial	Axial	Coronal	Axial
TR (millisecond)	544	3800	3300	8400
TE (millisecond)	10	72	55	63
Acquisition matrix	320×224	320×224	320×224	160×160
Field of view (cm)	220×220	200×200	200×200	220×220
Slice thickness (mm)	3	3	3	3
Increment(mm)	0.3	0.3	0.3	0.6
Flip angle (°)	150	127	160	180
Acquisition time(min)	2:12	2:40	2:12	3:47

using Statistical Package for Social Sciences (SPSS) version 21.0 (IBM Corporation, Armonk, NY, USA). Continuous variables were subjected to Student's *t* test or the nonparametric Friedman test, with a difference of $P < 0.05$ considered statistically significant.

Results

Patients

Of the 52 patients (males, 29; females, 23; mean age, 46.45±9.50 years), all patients underwent biochemical confirmation of SHPT, and none had undergone previous PTx, resulting in a total of 198 lesions identified intraoperatively. After excluding examinations with artifacts, all patients received preoperative MRI, compared with 45, 41, and 10 patients who also had 4D-CT, US, and ^{99m}Tc-sestamibi (MIBI), respectively (33 of whom preoperatively received both 4D-CT, US and MRI imaging modalities). The patients' baseline demographics and clinical characteristics are summarized in Table 2.

Radiologic Findings

General Analyses

The sensitivity, specificity, PPV and NPV of MRI, 4D-CT, and US are listed on a per-parathyroid gland basis in Table 3 and Table 4. Table 5 shows the performance of combined imaging modalities in 33 patients with renal hyperparathyroidism.

Table 2 Comparison of Demographics and Clinical Characteristics

Variable	Overall	MRI	4D-CT	US	*p*
NO. of patients	52	52	45	41	-
Gender (male/female)	29/23	29/23	24/21	22/19	0.24
Age (years)	46.45±9.50	46.45±9.50	45.71±9.42	47.10±9.57	0.86
Months of dialysis	130.12±5.47	130.12±5.47	130.32±4.15	131.52±6.27	0.92
BMI (kg/m^2)	23.31±7.12	23.31±7.12	23.21±7.62	23.03±6.42	0.976
Operation time (min)	86.53±16.62	86.53±16.62	87.37±15.6	85.67±17.46	0.56
Parathyroid min diameter (mm)	5*3	8*3	5*5	5*3	-
Nodular thyroid(n)	31	15	10	28	-
Less than 4 glands(patient, n)	5	5	4	4	-
Preoperative iPTH (pmol/L)	196.51±54.23	196.51±54.23	191.93±40.18	182.26±58.24	0.78
Preoperative Calcium (mmol/L)	2.50±0.53	2.50±0.53	2.49±0.28	2.48±0.78	0.67
Preoperative Phosphorus (mmol/L)	2.09±0.82	2.09±0.82	2.09±0.54	2.08±0.78	0.85
Preoperative ALP(U/L)	203.17±56.64	203.17±56.64	202.68±47.16	202.24±66.32	0.43

Notes: Values are expressed as n or mean ± standard deviation. $P > 0.05$ indicates there was no statistically significant difference.
Abbreviations: BMI, body mass index; iPTH, intact parathyroid hormone; ALP, alkaline phosphatase.

Table 3 All Patients, per-Parathyroid Gland (52 Patients, 198parathyroids)

	4D-CT (n=45)		MRI (n=52)		US (n=41)		*p*
	Rate(%)	95% CI	Rate(%)	95% CI	Rate(%)	95% CI	
Sensitivity	88.95	84.22–93.69	90.91	85.81–94.19	66.23	58.68–73.79	<0.001
Specificity	58.33	25.62–91.05	63.64	29.74–97.53	50	24.41–75.59	0.455
PPV	95.63	92.42–98.83	97.83	96.70–99.95	91.89	86.73–97.05	0.753<
NPV	26.92	8.65–45.19	28	826–43.59	14.75	5.60–23.91	0.185
AUC	0.736	0.525–0.908	0.766	0.594–0.938	0.581	0.439–0.724	<0.001

Abbreviations: CI, confidence interval of the difference; NPV, negative predictive value; PPV, positive predictive value; 4D-CT, four-dimensional computed tomography; MRI, magnetic resonance imaging; US, ultrasonography.

Table 4 Patients Received Both 3 Imaging Modalities, per-Parathyroid Gland (33 Patients, 126 parathyroids)

	Sensitivity (95% CI)	Specificity (95% CI)	PPV (95% CI)	NPV (95% CI)	AUC	*p*
4D-CT	85.94% (79.83–92.04)	50.00% (5.31–94.69)	96.49% (93.06–99.92)	18.18% (0.68–35.69)	0.718 (0.517–0.919)	$p < 0.001$ vs all others
MRI	88.10% (82.36–93.83)	55.56% (15.04–96.07)	95.69% (91.94–99.44)	25.00% (4.21–45.79)	0.680 (0.463–0.696)	
US	61.90% (53.31–70.50)	35.71% (7.00–64.42)	89.66% (83.13–96.18)	9.43% (1.30–17.57)	0.488 (0.329–0.647)	

Abbreviations: CI, confidence interval of the difference; NPV, negative predictive value; PPV, positive predictive value; 4D-CT, four-dimensional computed tomography; MRI, magnetic resonance imaging; US, ultrasonography.

Table 5 Performance of Combined Imaging Modalities in 33 Patients with Renal Hyperparathyroidism

	4D-CT+US		MRI+US		4D-CT+MRI		4D-CT+US+MRI		*p*
	Rate(%)	95% CI	Rate(%)	95% CI	Rate(%)	95% CI	Rate(%)	95% CI	
Sensitivity	85.94	79.83–92.04	88.1	82.36–93.83	88.1	82.36–93.83	88.1	82.36–93.83	0.938
Specificity	30.77	1.74–59.80	35.71	7.00–64.42	50	5.31–94.59	35.71	7.00–64.42	0.225
PPV	92.5	87.72–97.28	95.69	91.94–99.44	96.52	93.12–99.92	95.69	91.94–99.44	0.507
NPV	18.18	0.68–35.69	25	4.21–45.79	21.05	0.86–41.42	25	4.21–45.79	0.94

Abbreviations: CI, confidence interval of the difference; NPV, negative predictive value; PPV, positive predictive value; 4D-CT, four-dimensional computed tomography; MRI, magnetic resonance imaging; US, ultrasonography.

MRI outperformed both 4D-CT and ultrasonography, displaying greater sensitivity (MRI, 90.91%; 4D-CT, 88.95%; US, 66.23%), specificity (MRI, 63.64%; 4D-CT, 58.33%; US, 50.00%), PPV (MRI, 97.87%; 4D-CT, 95.63%; US, 91.89%) and NPV (MRI, 28.00%; 4D-CT, 26.92%; US, 14.75%). Receiver operating characteristic (ROC) analysis revealed that MRI had the highest performance for the detection of abnormal parathyroid lesions in patients with SHPT (area under the ROC curve [AUC] 0.766, 95% CI 0.594–0.938). The ORs of MRI, 4D-CT and US were 15.75, 11.67 and 1.96, and the AUCs of 4D-CT and US were 0.736 and 0.581, respectively (Table 3).

With regard to the performance of each imaging technique for 33 patients who preoperatively received all 3 imaging modalities, MRI was also significantly more sensitive (88.10%) and specific (55.56%) than all the other modalities studied in a per-parathyroid gland analysis ($P < 0.001$; Table 4). The specificities of 4D-CT and US were 55.56% and 35.71%, respectively.

In regard to combinations of modalities, as shown in, Table 5 the sensitivity of combined MRI and US (88.10%) was the highest among the combined 2 modalities. The combination of 4D-CT and US had the lowest sensitivity (85.94%), but there was no significant difference ($P > 0.05$) when the combination of 4D-CT and US was compared to the combination of 4D-CT and MRI.

Thirty-five percent of the patients had a nodular thyroid gland based on the findings on all 3 imaging modalities or their combinations. Thyroid nodules measuring more than 10 mm were identified in 3 patients (a solitary nodule in 2 patients and multiple nodules in 1 patient), and the thyroid gland was heterogeneous in 2 patients. There were no statistically significant differences in sensitivity of any of the three imaging modalities with respect to thyroid morphology, size of the HPG, blood PTH or Ca^{2+} levels (data not shown).

Subgroup Analyses

Among patients who received all 3 imaging modalities (n = 33), MRI identified 112 lesions, while 4D-CT and US identified 109 and 78 lesions, respectively. The mean [SD] diameters for the lesions precisely localized by MRI, 4D-CT and US were 13.32 mm [6.53], 15.45 mm [5.98] and 14.62 mm [7.28], respectively (p = 0.783). MRI missed 15, 127 lesions compared with 18, 127 lesions by 4D-CT and 49, 127 by US. There were 16 false-negative 4D-CT studies. In 4 patients (total 15 glands), MRI found all the glands, but CT or US could not. In the patients with fewer than 4 glands (n = 5), MRI correctly identified 14 of 15 parathyroid glands. Both US and 4D-CT were able to locate 12 parathyroid glands. The smallest diameter of the parathyroid gland precisely localized by MRI was 8×3 mm, 5×5 mm by 4D-CT, and 5×3 mm by US.

In 10 patients who also underwent ^{99m}Tc-MIBI scintigraphy, 12 abnormal parathyroid glands were correctly identified (positive rate was 28.57%), and this rate was lower than that of US. 99mTc-MIBI scintigraphy, which found that 1 patient had an ectopic parathyroid gland in the anterior mediastinum.

For ectopic parathyroid glands, 10 (19.2%) of the 52 patients had parathyroid lesions in ectopic locations: 4 in the superior mediastinum, 2 in the carotid sheath, 1 in the tracheoesophageal groove, 1 in the sternocleidomastoid muscle, 3 in the anterior cervical muscle, and 2 ectopic parathyroid glands located in the left lateral lobe of the thyroid gland (Table 6). Four ectopic mediastinal parathyroid glands (~1 to 2 cm) in patients 1, 2 and 3 were both localized by MRI, although 99mTc-MIBI precisely localized a lesion in the right superior mediastinum in 1 patient (Figure 1). There was 1 ectopic parathyroid gland at the left tracheoesophageal groove at the level of the T2 vertebra; however, only MRI was successful in localizing the lesion in this patient (patient 9; size, ~1.0 cm). Two patients had ectopic parathyroid glands at the left carotid sheath region (patients 4 and 6), one of which was correctly localized by MRI and 4D-CT (patient 4; size, ~1.5 cm); however, only the operation was successful in localizing this rather small hyperplastic parathyroid lesion (patient 6; size, ~0.5 cm).

Outcomes

All 52 patients were confirmed to have parathyroid hyperplasia with postoperative pathology. With 6-month post-operative follow-up data, 48 achieved biochemical cure (92.3%), including one patient with a correctly lateralized lesion by MRI (5 parathyroid lesions) (Figure 2). The mean serum calcium level was 2.20±0.32 mmol/L, and the median serum PTH level was 6.04 (2.45, 17.33) pmol/L. One patient with mediastinum-located ectopic PTG in our cohort underwent reoperation (superselective embolization for PTG vascular) and eventual cure (patient 1). One patient underwent surgery to remove all lesions preoperatively located by imaging modalities without delineating the PTH level (184pg/mL) 3 months after the operation. Then, with the introduction of 99mTc-Sestamibi SPECT/CT imaging into our hospital, we applied the new imaging technology to the case and discovered an ectopic parathyroid gland hidden in the superior mediastinum (patient 3, Table 6). Perhaps further hyperplasia of the gland makes it more visible by imaging. The remaining patients underwent further workup prior to reoperation. Of all the operations, hematoma requiring operative evacuation occurred in 1 patient (1.9%), and postoperative hypoparathyroidism was seen in three patients (5.8%) at or beyond 6 months after the operation.

Discussion

On a lesion-based analysis, this study, for the first time, compared the diagnostic performance of MRI, 4D-CT, ultrasonography and ^{99m}Tc-MIBI in the preoperative workup in patients with SHPT. The strength of the study is the comparative statistical approach for correlating proportions of clustered data, which were prospectively collected.

We found significantly better stand-alone performance of MRI regarding sensitivity, specificity, positive predictive value (PPV) and negative value of prediction (NPV) compared with all the other modalities investigated. If MRI cannot be implemented, 4D-CT can be an alternative to locate parathyroid glands preoperatively. In 33.3% (5/15) of cases, ectopic parathyroid gland anatomic lesions that could not be confirmed by US or 4D-CT were successfully localized using MRI, thus enabling tPTX+AT.

In patients who require parathyroidectomy, tPTX+AT has become increasingly the first choice in many clinical centers,[13,14] although total parathyroidectomy (tPTX) has also been proposed for refractory SHPT.[15] Regardless of the procedures, precise preoperative localization of abnormal parathyroid glands may be very useful to prevent recurrent or persistent disease and to perform more rapid and meticulous surgery in high-risk patients with renal failure or a kidney graft.[16] Especially for reoperation, the risk of recurrent laryngeal nerve injury could rise from <1% to 15% −18.8%.[17,18] Noninvasive imaging tests include MR, CT, US imaging, and scintigraphic methods, such as ^{99m}Tc-MIBI. The reported sensitivities for these techniques in this setting vary. Nevertheless, to our knowledge, studies have systematically investigated the performance of the above four imaging modalities in SHPT simultaneously.[19,20]

A wide range of diagnostic accuracies of US and ^{99m}Tc-MIBI has previously been reported. Accordingly, Lee found an overall sensitivity for preoperatively detecting abnormal sHPG by US of 91.5%, 56.1% for ^{99m}Tc-MIBI, and 93.8% for the combination of US with ^{99m}Tc-MIBI.[21] Sophie showed that US detected 75% of the hyperplastic glands, while

Table 6 Results of MRI, 4D-CT, US and 99mTc-MIBI in 10 Patients with Ectopic PTGs, Related to Surgical and Pathological Findings

S/No	Age, y/Sex	MRI	4D-CT	US	^{99m}Tc-MIBI	Preop PTH (pmol/L)	Intraoperative p PTH (pmol/L)	Surgery and Pathological Findings
1	54/Male	Right P3 Left P3 Ectopic (mediastinum) Left thyroid nodule	Right P3 Left P3	Right P3 Left P3 No detectable Right/left P4	Right P3 Left P3 One ectopic (mediastinum)	177	25	Hp right P3 (15*13mm) Hp left P3 (20*15mm) Ectopic Hp (25*20mm) Left thyroid lobe, no cancer
2	49/Male	Right P4 Left P3 Left P4 Ectopic (mediastinum)	–	Right P3 Right P4 Left P3	No image of parathyroid gland	378	1.8	Hp right P4 (10*10mm) Hp left P3 (15*15mm) Hp left P4 (10*12mm) Ectopic Hp (10*10mm
3	56/Male	Right P4 Left P4 Two ectopic (mediastinum)	–	Right P4 Left P4 Thyroid cyst in the right lobe	–	184.44	89.9	Hp right P4 (10*10mm) Hp left P4 (15*10mm) Ectopic Hp (8*12mm, left) Right ectopic PTGs cannot be removed due to very low position
4	38/Male	Right P4 Ectopic (Sternocleidomastoid muscle +anterior cervical muscle +Left carotid sheath)	Right P4 Left P3 Ectopic (two in sternocleidomastoid muscle+Left carotid sheath)	Right P4 Left P3	No image of parathyroid gland	442	11	Hp right P4 (15*21mm) Ectopic Hp (Sternocleidomastoid muscle 20*20mm+anterior cervical muscle 15*20mm +Left carotid sheath 15*16mm)
5	38/female	–	Ectopic (Two in anterior cervical muscle+left lateral lobe of the thyroid gland)	–	No image of parathyroid gland	138	5.2	Ectopic Hp (anterior cervical muscle 10*6mm□5*5mm + left lateral lobe of the thyroid gland 5*6mm)
6	44/female	Right P4 Right P3 Left P3	Right P3 Left P3	Right P4 Right P3 Left P3	–	348	1.9	Hp right P4 (10*15mm) Hp right P3 (30*15mm) Hp left P3 (10*15mm) Ectopic Hp (5*5mm)
7	45/female	Right P4 Right P3 Left P3 Ectopic (left lobe of the thyroid gland)	Right P4 Right P3 Left P3	Right P4 Right P3 Left P3	No image of parathyroid gland	178	17	Hp right P4 (20*15mm) Hp right P3 (20*12mm) Hp left P3 (20*25mm) Ectopic Hp (10*10mm)

(*Continued*)

https://doi.org/10.2147/TCRM.S379814 DovePress

Table 6 (Continued).

S/No	Age, y/Sex	MRI	4D-CT	US	^{99m}Tc-MIBI	Preop PTH (pmol/L)	Intraoperative p PTH (pmol/L)	Surgery and Pathological Findings
8	46/female	Right P4 Left P3 Left P4	Right P4 Right P3 Left P4 Ectopic lobe of the thyroid gland)	Doubt intrathyroidal Right P4 or right Thyroid nodule	–	267	4.7	Hp right P4 (30*15mm) Hp right P3 (20*15mm) Hp left P3 (5*3mm) Ectopic Hp (30*20mm) multinodular goiter with calcification in the left lobe thyroid nodule including two papillary carcinomas (5mm each)
9	40/female	Right P4 Left P4 Left P3 Ectopic (tracheoesophageal groove)	Right P4 Left P4 Left P3	Left P4 Right P4	–	210	2.5	Hp right P4 (10*5mm) Hp Left P4 (10*6mm) Hp left P3 (20*15mm) Ectopic Hp (left tracheoesophageal groove 10*8mm)
10	44/female	Right P4 Right P3 Ectopic (left lateral lobe of the thyroid gland)	Right P4 Right P3	Right P4 Right P3 Left P4	–	279	39	Hp right P4 (18*25mm) Hp right P3 (20*15mm) Ectopic Hp (left lateral lobe of the thyroid gland 25*15mm)

Abbreviations: Hp, hyperplastic parathyroid gland; PTGs, parathyroid glands; HPT, hyperparathyroidism; P, parathyroid gland; P3, inferior P; P4, superior P.

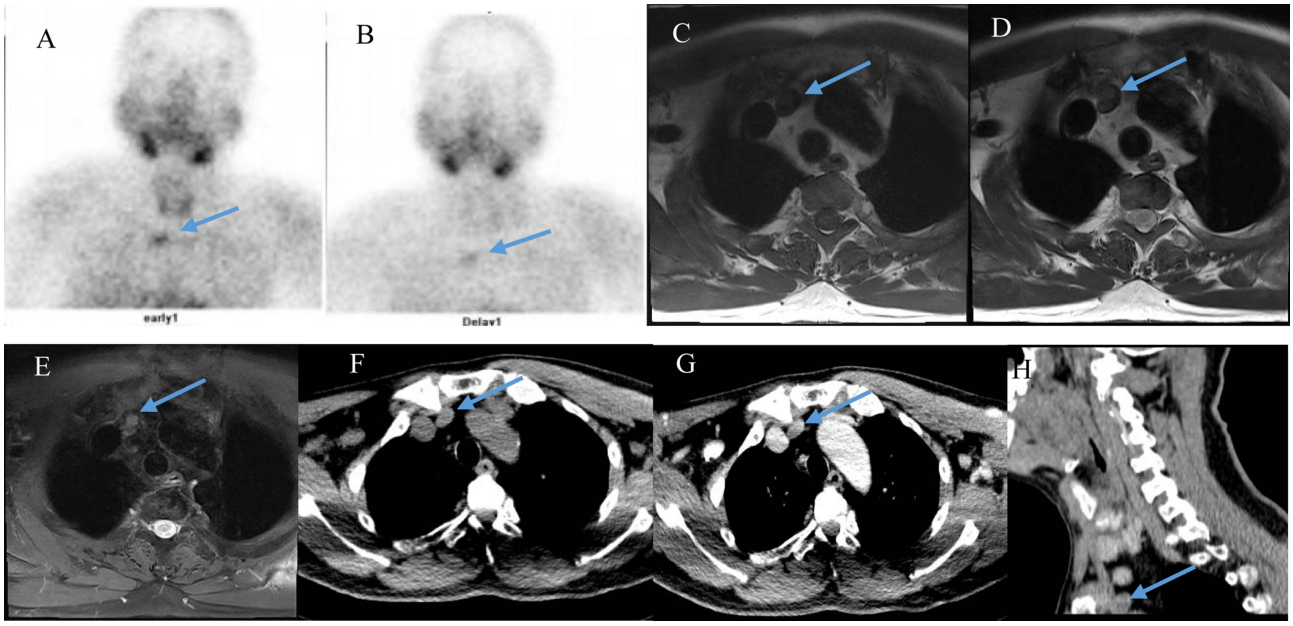

Figure 1 Patient1: Dual-phase 99mTc-setaMIBI planar images at early 10 minutes and delayed 2 hours (**A** and **B**) reveal tracer high uptake. MRI images (**C**–**E**) and CT transaxial, and sagittal images (**F**–**H**) shows a lesion in the right side of superior mediastinum (arrow).

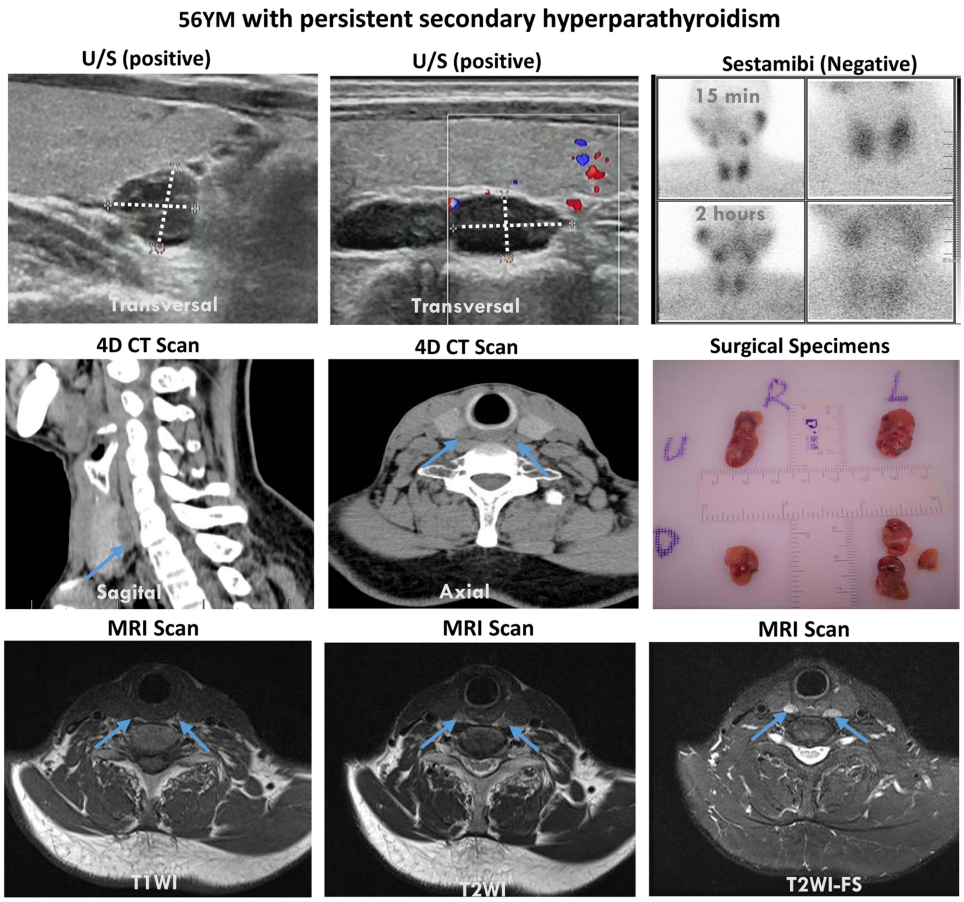

Figure 2 Secondary hyperparathyroidism in a 56-year-old dialysed patient. A dual-phase 99m Tc-MIBI imaging was nonlocalizing, MRI and high-resolution ultrasonography was both suggestive of five enlarged parathyroid glands. 4D-CT revealed a 1.3 cm retroesophageal parathyroid adenoma posterior to the cricoid cartilage, located superior the right thyroid glands (an arrow). Even the left inferior parathyroid gland, which was the smallest in size and weight, was found during surgery and hyperplastic parathyroid gland was verified by postsurgical histology in all lesions. PTH serum levels decreased from 170 pg/mL preoperatively to 24 pg/mL on the day after surgery.

^{99m}Tc-MIBI identified 66%.[22] The combination of both modalities identified 88% of the glands. Furthermore, a recent retrospective study investigating preoperative localization techniques in SHPT reported a pooled sensitivity for US, ^{99m}Tc-MIBI, and combined techniques of 62%, 55%, and 73%, respectively,[8] with significant heterogeneity between the studies. Although we achieved a comparable sensitivity (64.17% or 71.13%) using US in parathyroid gland localization to these reports, the sensitivity with MIBI was surprisingly lower in our study (28.57%) than the usual range of 44% −77% in patients with hyperplasia,[20,23] except for the results from a team that reported greater values (91%).[24] Due to its high sensitivity, particularly its ability to distinguish parathyroid from thyroid lesions, ^{99m}Tc-MIBI is highly recommended by many scholars as the first-line modality for imaging SHPT, especially MGD. However, it should be used in conjunction with another modality to improve diagnostic efficiency.[25] The surprisingly poor performance of ^{99m}Tc-MIBI is in contrast to many previous findings; however, patient 4 underwent surgery to remove all lesions preoperatively located by imaging modalities, including MIBI, in patients who still had high serum PTH levels (220 pg/mL) after TPTX. Subsequent ^{99m}Tc-Sestamibi SPECT/CT imaging at our hospital revealed 1 lesion in the right sternocleidomastoid muscle at the level of the T1 vertebra. Conversely, worse diagnostic performance of ultrasonography was also achieved in patients with secondary and tertiary hyperparathyroidism, with a sensitivity range of 24% to 54% (28–31).[24,26] The poor performance of ultrasonography may be due to the poor distinction of parathyroid glands and lymph nodes from doctors and the sensitivity of the inspection equipment.

Ultrasonography has been increasingly used to localize parathyroid glands, not least due to its accessibility, low cost, and nonionizing properties. However, the disadvantages of US include operator dependence and limited fields of view; the latter is particularly troublesome when ectopic glands in the mediastinum are considered.[27] Rodgers[28] also found US and MIBI imaging methods to be unsuitable for patients in the aftermath of neck surgery or in conjunction with thyroid disease and unfavorable body conditions.[29] In 2006, 4D-CT was introduced as a contrast-based CT protocol with multiplanar images exploiting differences in perfusion characteristics over time to precisely localize abnormal parathyroid glands.[30] Rodgers et al first reported sensitivities of 88 and 70% of 4D-CT for lateralization and localization in primary hyperparathyroidism, respectively.[28] To date, there is a paucity of literature examining the role of 4D-CT in patients with secondary hyperparathyroidism. More recently, other authors have shown that 4D-CT had an adequate utility of detecting abnormal parathyroid glands in SHPT enlarged parathyroid glands in SHPT.[21] A study performed in 109 Korean patients investigating preoperative localization techniques in secondary HPT reported high sensitivity (84.8%) with the use of 4D-CT.[22] In a retrospective study by Takagi,[31] 4D-CT also showed impressive results and performed better than sestamibi SPECT or US, which is not surprising, as this is in accordance with our studies, and that study demonstrated a comparable sensitivity of 85.04% in multiple hyperplastic parathyroid glands and a specificity of 28.57%. However, Giron showed that the sensitivity of multiple hyperplastic parathyroid glands was 59%, which was lower than that in our study.[19]

MRI has also been extensively used for hyperplastic parathyroid glands in SHPT. In our study of 33 patients with 127 surgically verified hyperplastic parathyroid glands, both MRI imaging and 4D-CT imaging were consistent with the surgical findings in 127 lesions. In 4 lesions, neither imaging study was concordant (false-positive) with the surgical findings. However, in the remaining patient, MRI correctly identified 4 parathyroid lesions that were missed by 4D-CT or US. Giron[19] studied patients with secondary hyperparathyroidism before repeated surgery using MRI, CT, US, and ^{99m}Tc-MIBI scintigraphy and showed that associated and complementary tests, morphological and functional, MRI (fat-salt, T1, gadolinium) and ^{99m}Tc-MIBI, have greater efficacy. In their preliminary analysis, the sensitivity for MRI and MIBI of the neck was 69% and 70%, respectively, whereas a sensitivity of 75% with 8% false positives was observed when the two imaging modalities were coupled.[19] Wada[23] evaluated the utility of MRI imaging and ^{99m}Tc-MIBI scintigraphy in the precise localization of abnormal parathyroid glands before and after percutaneous ethanol injection therapy (PEIT) in a study of 24 patients with SHPT. Among the small parathyroid glands (<0.5 mL with US), the lesion-based sensitivity for MRI was significantly better than that for ^{99m}Tc-MIBI imaging (74% vs 40%). However, MR images and MIBI showed similar detectability (95% vs 90%) for large parathyroid glands (> or = 0.5 mL with US). Moreover, the specificity of MR imaging was much higher (100%) than that of MIBI scintigraphy in evaluating therapeutic effects. The studies of Wada and Giron both showed better ^{99m}Tc-MIBI sensitivity than the results obtained with ^{99m}Tc-MIBI that we obtained.[19,23] However, all 3 studies, including our study, showed considerable sensitivity with MRI.[19,23] However,

other authors have reported sensitivities of MR imaging, including SHPT patients and recurrent or persistent HPT patients, of 57–88%.[19,20,27,32–34] A further refinement of MR imaging equipment, techniques and image analysis software, as well as increased investigator experience, are likely responsible for the improved sensitivities in recent studies[34,35] compared with older data.[19,33] Although 4D-CT and MR imaging both provide excellent anatomic detail, superior tissue contrast, ability to image vasculature without the need for contrast material, lack the need for ionizing radiation, have multiplanar capability, have superiority in identifying ectopic and small parathyroid lesions, and have relatively minimal artifact surrounding surgical clips in the neck make MR imaging preferable to CT scanning in this patient population.

Approximately 5–20% of parathyroid glands are ectopic,[19,36,37] a situation that is even more frequent in patients with recurrent or persistent sHPT after failed neck explorations. Abnormal ectopic parathyroid tissue was found as the cause of recurrent or persistent sHPT in our series in 4 (7.7%) of 52 patients or in 15 (7.4%) of all 198 resected glands. MR imaging demonstrated excellent sensitivity for the detection of these lesions and helped identify 83.3% (10 of 12) of such glands (patient 5 received CT scanning that revealed 3 ectopic parathyroid glands but refused subsequent MR imaging because of financial problems). Furthermore, the observed higher sensitivity of MRI compared with US and 4D-CT could largely be due to its increased ability to detect ectopic lesions. Other investigators have also observed that 99mTc-sestamibi imaging should be used initially to localize the ectopic parathyroid glands in patients with hyperparathyroidism for anatomical guidance prior to MR or CT imaging.[34]

The study has the following limitations: Not all patients completed MRI, 4D-CT, and US examinations. Only 10 patients completed MIBI due to worries about radiation, reagent orders and equipment maintenance. An insufficient sample size is also a shortcoming of this study. In addition, due to the introduction of new technology, we will compare SPECT and MRI in the future.

In view of the experience acquired during this study, we propose the following real-world strategy. Ultrasonography is performed first because of its accessibility, low cost, and nonionizing properties. Most importantly, it achieved a relatively high sensitivity to the initial localization of abnormal parathyroid glands. MRI is performed subsequently with knowledge of ultrasonography results and because of its largest field of view. The radiologist is guided to areas with suspicious parathyroid tissue, and MRI adds useful anatomic data for the surgeon that may limit exploration and increase the surgical success rate.

Conclusions

Our retrospective analysis concluded that although ultrasonography is not highly sensitive for the diagnosis of secondary parathyroid hyperplasia (only at least one hyperplastic gland needs to be found), it can be considered the first choice for the diagnosis of the disease due to economic, nonradiation and other reasons. However, before total parathyroid resection, it is possible to locate all parathyroid glands to reduce the operation time and increase the success rate of surgery. MRI has more advantages than CT.

Data Sharing Statement

The data sets generated and/or analyzed during the current study are not publicly available but are available from the corresponding author on reasonable request.

Ethical Approval

All procedures performed in studies involving human participants were in accordance with the ethical standards of the institutional and/or national research committee and with the 1964 Helsinki declaration and its later amendments or comparable ethical standards. This study was approved by ethical board of The Fifth Affiliated Hospital of Sun Yat-sen University. Informed consent was obtained from all individual participants included in the study and all the study participants gave consent to publish.

Acknowledgments

The authors would like to thank Dr. Yunping Fan for his assistance in performing the surgery.

Funding

This study was supported by a grant from the Zhuhai Scientific and Technological Project Fund (No. 20181117E030007). Guangdong administration of Traditional Chinese Medicine Project Fund (No.20191072). Guangdong Medical research fund (No. A2020364).

Disclosure

The authors have no conflicts of interest to declare.

References

1. Goodman WG, Goldin J, Kuizon BD, et al. Coronary-artery calcification in young adults with end-stage renal disease who are undergoing dialysis. *New England J Med*. 2000;342:1478–1483. doi:10.1056/NEJM200005183422003
2. Fraser WD. Hyperparathyroidism. *Lancet*. 2009;374:145–158. doi:10.1016/S0140-6736(09)60507-9
3. Lun L, Liu D, Gao Z, et al. Effects of parathyroidectomy on quality of life in remic patients with secondary hyperparthyroidism. *Chin J Blood Purifc*. 2014;29:270.
4. Noussios G, Anagnostis P, Natsis K. Ectopic parathyroid glands and their anatomical, clinical and surgical implications. *Exp Clin Endocrinol Diabetes*. 2012;120:604–610. doi:10.1055/s-0032-1327628
5. Gough I. Reoperative parathyroid surgery: the importance of ectopic location and multigland disease. *ANZ J Surg*. 2007;76:1048–1050. doi:10.1111/j.1445-2197.2006.03931.x
6. Ulanovski D, Feinmesser R, Cohen M, et al. Preoperative evaluation of patients with parathyroid adenoma: role of high-resolution ultrasonography. *Head Neck*. 2002;24(1):1–5. doi:10.1002/hed.10043
7. Huppert BJ, Reading CC. Parathyroid sonography: imaging and intervention. *J Clin Ultrasound*. 2007;35:144–155. doi:10.1002/jcu.20311
8. Carlo V, Maurizio B, Annamaria D, et al. Usefulness of the combination of ultrasonography and 99mTc-sestamibi scintigraphy in the preoperative evaluation of uremic secondary hyperparathyroidism. *Head Neck*. 2010;32:1226–1235. doi:10.1002/hed.21320
9. Lappas D, Noussios G, Anagnostis P, et al. Location, number and morphology of parathyroid glands: results from a large anatomical series. *Anat Sci Int*. 2012;87:160–164. doi:10.1007/s12565-012-0142-1
10. Perrier N. Four-dimensional computed tomography: clinical impact for patients with primary hyperparathyroidism. *Ann Surg Oncol*. 2017;25:17. doi:10.1245/s10434-017-6117-7
11. Sacconi B, Argirò R, Diacinti D, et al. MR appearance of parathyroid adenomas at 3T in patients with primary hyperparathyroidism: what radiologists need to know for pre-operative localization. *Eur Radiol*. 2016;26:664–673. doi:10.1007/s00330-015-3854-5
12. Frunzac RW, Richards M. Computed tomography and magnetic resonance imaging of the thyroid and parathyroid glands. *Front Horm Res*. 2016;45:16–23.
13. Naranda J, Ekart R, Pečovnik-Balon B. Total parathyroidectomy with forearm autotransplantation as the treatment of choice for secondary hyperparathyroidism. *J Int Med Res*. 2011;39:978–987. doi:10.1177/147323001103900333
14. Magnabosco FF, Tavares MR, Montenegro FL. Surgical treatment of secondary hyperparathyroidism: a systematic review of the literature. *Arq Bras Endocrinol Metabol*. 2014;58:562–571. doi:10.1590/0004-2730000003372
15. Qiu NC, Zha SL, Liu ME, et al. To assess the effects of parathyroidectomy (TPTX versus TPTX+AT) for Secondary Hyperparathyroidism in chronic renal failure: a meta-analysis. *Int J Sur*. 2017;44:353–362. doi:10.1016/j.ijsu.2017.06.029
16. Mi JP, Liao ZP, Pei XF, et al. Postsurgical evaluation of secondary nephrogenic hyperparathyroidism. *Curr Med Sci*. 2019;39:259–264. doi:10.1007/s11596-019-2028-0
17. Karakas E, Müller H-H, Schlosshauer T, Rothmund M, Bartsch DK. Reoperations for primary hyperparathyroidism- improvement of outcome over two decades. *Langenb Arch Surg*. 2013;398:99–106. doi:10.1007/s00423-012-1004-y
18. Scappaticcio L, Maiorino MI, Iorio S, et al. Thyroid surgery during the COVID-19 pandemic: results from a systematic review. *J Endocrinol Invest*. 2022;45(1):181–188. doi:10.1007/s40618-021-01641-1
19. Giron J, Ouhayoun E, Dahan M, et al. Imaging of hyperparathyroidism: US, CT, MRI and MIBI scintigraphy. *Eur J Radiol*. 1996;21:167–173. doi:10.1016/0720-048X(95)00711-X
20. Ishibashi M, Nishida H, Okuda S, et al. Localization of parathyroid glands in hemodialysis patients using Tc-99m sestamibi imaging. *Nephron*. 1998;78:48–53. doi:10.1159/000044882
21. Lee JB, Kim WY, Lee YM. The role of preoperative ultrasonography, computed tomography, and sestamibi scintigraphy localization in secondary hyperparathyroidism. *An Surg Treat Res*. 2015;89:300–305. doi:10.4174/astr.2015.89.6.300
22. Périé S, Fessi H, Tassart M, et al. Usefulness of combination of high-resolution ultrasonography and dual-phase dual-isotope iodine 123/technetium Tc 99m sestamibi scintigraphy for the preoperative localization of hyperplastic parathyroid glands in renal hyperparathyroidism. *Am J Kidney Dis*. 2005;45:344–352. doi:10.1053/j.ajkd.2004.10.021
23. Wada A, Sugihara M, Sugimura K, et al. Magnetic Resonance Imaging (MRI) and Technetium-99m-methoxyisonitrile (MIBI) scintigraphy to evaluate the abnormal parathyroid gland and PEIT efficacy for secondary hyperparathyroidism. *Radiat Med*. 1999;17:275.
24. Jeanguillaume C, Urea P, Hindié E, et al. Secondary hyperparathyroidism: detection with I-123-Tc-99m-sestamibi subtraction scintigraphy versus US. *Radiology*. 1998;207:207–213. doi:10.1148/radiology.207.1.9580138
25. Wakamatsu H, Noguchi S, Yamashita H, et al. Parathyroid scintigraphy with 99mTc-MIBI and 123I subtraction: a comparison with magnetic resonance imaging and ultrasonography. *Nucl Med Commun*. 2003;24:755–762. doi:10.1097/00006231-200307000-00004
26. Light V, Mhenry C, Jarjoura D, Sodee D, Miron S. Prospective comparison of dual-phase technetium-99m-sestamibi scintigraphy and high resolution ultrasonography in the evaluation of abnormal parathyroid glands. *Am Surg*. 1996;62:567–568.
27. Numerow LM, Morita ET, Clark OH, Higgins CB. Persistent/recurrent hyperparathyroidism: a comparison of sestamibi scintigraphy, MRI, and ultrasonography. *J Magn Reson Imaging*. 1995;5:702–708. doi:10.1002/jmri.1880050614

28. Rodgers SE, Hunter GJ, Hamberg LM, et al. Improved preoperative planning for directed parathyroidectomy with 4-dimensional computed tomography. *Surgery*. 2006;140:932–940. doi:10.1016/j.surg.2006.07.028
29. Suh YJ, Choi JY, Kim SJ, et al. Comparison of 4D CT, Ultrasonography, and 99mTc Sestamibi SPECT/CT in localizing single-gland primary hyperparathyroidism. *Otolaryngol Head Neck Surg*. 2015;152:438–443. doi:10.1177/0194599814562195
30. Lubitz C, Hunter G, Hamberg L, et al. Accuracy of 4-dimensional computed tomography in poorly localized patients with primary hyperparathyroidism. *Surgery*. 2010;148:1129–1137. doi:10.1016/j.surg.2010.09.002
31. Takagi H, Tominaga Y, Uchida K, et al. Image diagnosis of parathyroid glands in chronic renal failure. *Ann Surg*. 1983;198:74–79. doi:10.1097/00000658-198307000-00015
32. Fayet P, Hoeffel C, Fulla Y, et al. Technetium-99m sestamibi scintigraphy, magnetic resonance imaging and venous blood sampling in persistent and recurrent hyperparathyroidism. *Br J Radiol*. 1997;70:459–464. doi:10.1259/bjr.70.833.9227226
33. Peeler BB, Martin WH, Sandler MP, Goldstein RE. Sestamibi parathyroid scanning and preoperative localization studies for patients with recurrent/persistent hyperparathyroidism or significant comorbid conditions: development of an optimal localization strategy. *Am Surg*. 1997;63:37–46.
34. Ishibashi M, Nishida H, Hiromatsu Y, et al. Comparison of Technetium-99m-MIBI, Technetium-99m-Tetrofosmin, Ultrasound and MRI for Localization of Abnormal Parathyroid Glands. *J Nucl Med*. 1998;39:320–324.
35. Gotway MB, Reddy GP, Webb WR, et al. Comparison between MR Imaging and 99m Tc MIBI scintigraphy in the evaluation of recurrent or persistent hyperparathyroidism. *radiology*. 2001;218:783. doi:10.1148/radiology.218.3.r01fe38783
36. Kang YS, Rosen K, Clark OH, Higgins CB. Localization of abnormal parathyroid glands of the mediastinum with MR imaging. *Radiology*. 1993;189:137–141. doi:10.1148/radiology.189.1.8372183
37. Akerstrom G, Malmaeus J, Bergstrom R. Surgical anatomy of human parathyroid glands. *Surgery*. 1984;95:14.